



The electrochemical synthesis of CNTs/N-Cu₂S composites as efficient electrocatalysts for water oxidation

Junjie Hou · Xuemei Zhou · Zhi Yang · Huagui Nie

Received: 30 January 2019 / Accepted: 6 December 2019 / Published online: 2 January 2020
© Springer Nature B.V. 2020

Abstract Oxygen evolution reaction (OER) catalysts are of central importance for electrocatalytic water oxidation and fuel generation, while it is still an urgent requirement to design and develop efficient OER catalysts with rapid kinetics and low overpotentials. Herein, we report an electrochemical deposition method to fabricate carbon nanotubes/N-doped cuprous sulfide (CNTs/N-Cu₂S) composites using thiourea and a CuSO₄ solution as the S and Cu sources, respectively. The advantages of this strategy include low cost, simple processing and the absence of templates or surfactants that can otherwise affect the electrochemical properties of the products. The N supplied by the thiourea can be used as a doping agent as a result of the in situ formation of small N-Cu₂S particles, which can increase larger surface area and create more active sites to enhance OER catalytic activity, compared with that obtained with materials synthesized without adding the thiourea. The synergic interface of CNTs and N-Cu₂S can improve conductivity and efficient chemical transfer in the

composites electrodes by introducing CNTs. Under the optimal experimental conditions, the CNTs/N-Cu₂S-5cyc composites present an excellent activity with the current density of 10 mA cm⁻² at a low OER overpotential of 280 mV, the Tafel slope of 63 mV dec⁻¹ and a strong electrochemical stability in 1.0 M KOH solution.

Keywords Cuprous sulfide · Carbon materials · Composites · Electro-deposition · Oxygen evolution reaction · Nanostructured catalyst

Introduction

The generation of O₂ via electrochemical water oxidation using the oxygen evolution reaction (OER) is of great importance as a means of converting and storing energy, and is also vital to metal–air batteries and water-splitting processes (Suen et al. 2017; Kanan et al. 2009; Nocera 2012; Dou et al. 2016). The oxidation of water at an anode is an energy-intensive reaction and requires a minimum initiation energy input of 1.23 V (vs a reversible hydrogen electrode, RHE). As such, OER kinetics tends to be sluggish and represents a critical bottleneck in the improvement of water-splitting technologies. An efficient OER electrocatalyst is required to provide a high current density at a low overpotential. Although Ir- and Ru-based catalysts show remarkable OER catalytic activities (Nakagawa et al. 2009; Over 2012), these metals are both rare and costly. Therefore, there is an

Electronic supplementary material The online version of this article (<https://doi.org/10.1007/s11051-019-4729-5>) contains supplementary material, which is available to authorized users.

J. Hou · X. Zhou · Z. Yang · H. Nie (✉)
Nanomaterials & Chemistry Key Laboratory, Wenzhou University, Wenzhou 325027, China
e-mail: huaguinie@126.com

X. Zhou (✉)
School of Material and Energy, Guangdong University of Technology, Guangzhou 510006, China
e-mail: zxm.mei@163.com

urgent requirement to design and develop efficient OER catalysts with rapid kinetics and low overpotentials.

A number of OER catalysts have been developed based on 3d metals such as Fe, Cu, Co, Ni and Mn. Examples include single- and mixed-metal oxides (hydroxides) (Subbaraman et al. 2012; Zhou et al. 2014; Zhou et al. 2015), chalcogenides (Yang et al. 2017a, b; Liu et al. 2015), phosphates (Li et al. 2016; Shen et al. 2016; Xie et al. 2017), borides (Chen et al. 2016), perovskites (Guo et al. 2015; Suntivich et al. 2011) and molecular catalysts (Brimblecombe et al. 2010). These materials are attractive due to their low cost, high chemical stability and good electrocatalytic activities. Among these, the copper sulfides (Cu_xS) have attracted significant interest, owing to their potential applications in many different fields, including catalysis (Tanveer et al. 2014), biosensing (Ku et al. 2013) and energy conversion and storage (Li et al. 2018; An et al. 2015). However, the majority of Cu-based catalysts exhibit high overpotentials and low current densities in OER systems. One approach to lowering the overpotential of such materials while increasing the current density is to introduce a conductive support, while also doping with a third element to create a hybrid system. Recently, a $\text{Cu}_2\text{S}/\text{C}$ electrode having a peapod-like structure showed enhanced electrocatalytic activity in conjunction with a low overpotential of 401 mV and a current density of 10 mA cm^{-2} in an alkaline solution (Zhao et al. 2017). Co-engineered Cu_7S_4 nanodisks have also demonstrated high activity and excellent durability in alkaline environments (Li et al. 2017). In addition, two-dimensional ultrathin $\text{Ni}(\text{OH})_2\text{-Cu}_2\text{S}$ hexagonal nanosheet hybrids have exhibited a current density of 10 mA cm^{-2} at an overpotential of 0.5 V and produced a Tafel slope of 89 mV dec^{-1} during water oxidation in 0.1 M KOH (Yang et al. 2017a). Such reports demonstrate that Cu_xS materials are a promising candidate for use in electrochemical energy conversion and storage systems. Even so, the electrocatalytic performance of these compounds remains inferior to those of state-of-the-art water-oxidation catalysts such as RuO_2 and IrO_2 . Additionally, the synthesis of Cu_xS still requires very harsh conditions that incorporate toxic organic solvents as well as surfactants, structure-directing agents and high temperatures. Therefore, the development of a simple and effective means of producing highly efficient Cu_2S OER catalysts is still required.

In the present work, a one-step electrochemical deposition method based on cyclic voltammetry (CV) was

developed for the fabrication of CNTs/N- Cu_2S composites. This new process employs thiourea and a CuSO_4 solution as the S and Cu sources, respectively. The advantages of this strategy include low cost, simple processing and the absence of templates or surfactants that can otherwise affect the electrochemical properties of the products. In addition, the N supplied by the thiourea can be used as a doping agent as a result of the in situ formation of small N- Cu_2S particles. The high surface area of such particles creates a large number of active sites, and so enhances the OER catalytic activity compared with that obtained with materials synthesized without adding the thiourea. Lastly, the electrical conductivity of the Cu_2S can be improved by introducing carbon nanotubes (CNTs) as the conductive substrate. The interface between these CNTs and the Cu_2S in the composite ensures both efficient charge transport and the rapid transfer of chemical species to the OER electrodes. As a result of these factors, the CNTs/N- Cu_2S -5cyc catalyst developed in this work delivers an OER overpotential as low as 280 mV at 10 mA cm^{-2} and a low Tafel slope of 63 mV dec^{-1} while showing good electrochemical stability in a 1.0 M KOH solution.

Experimental sections

Materials and reagents

Copper sulfate pentahydrate ($\text{CuSO}_4 \cdot 5\text{H}_2\text{O}$), potassium hydroxide (KOH), thiourea ($\text{CH}_4\text{N}_2\text{S}$, TH) and iridium oxides (IrO_2) were purchased from Shanghai Aladdin Biochemical Technology Co., Ltd. The carbon nanotubes (CNTs) were purchased from Cnano Technology (Beijing) Limited Company. Nafion (5 wt%) was obtained from Sigma-Aldrich, and all chemicals were used without further purification.

Synthesis of CNTs/N- Cu_2S Nanocomposites

The CNTs/N- Cu_2S composites were synthesized by a simple and convenient electrochemical deposition method. In a typical experiment, the electro-deposition measurement was carried out by a CV via a three-electrode system (PINE, Grove City, America). The CNTs-TH (the different mass ratio of CNTs and TH by mixing, marked as CNTs-TH) modified glassy carbon electrodes (GCEs) was used as the working electrode, platinum wires as the counter

electrode and Ag/AgCl (saturated-KCl) as the reference electrode, respectively. In order to obtain CNTs/N-Cu₂S nanocomposites, CNTs-TH-modified GCEs were dipped into 10-mM fresh CuSO₄·5H₂O solution and electrodeposited in the potential range from +0.8 to -0.6 V vs. Ag/AgCl, at a scan rate of 40 mV s⁻¹ with 5 CV cycles, which was labeled as CNTs/N-Cu₂S-5cyc. The parallel experiments were also carried out under the same conditions except for different deposition cycles (3, 10 and 15 CV cycles), which were denoted as CNTs/N-Cu₂S-3cyc, CNTs/N-Cu₂S-10cyc, CNTs/N-Cu₂S-15cyc, respectively. Besides, the CNTs/CuO-5cyc was gained with only CNTs (without adding TH) modified GCEs by exactly the same steps.

Structure characterization

The morphology and structure of the samples were observed by scanning electron microscopy (SEM, FEI Nova Nano SEM 200). Transmission electron microscopy (TEM), high-resolution transmission electron microscopy (HRTEM), scanning transmission electron microscopy (STEM) and corresponding elemental mapping and selected area electron diffraction (SAED) were recorded with a JEOL-2100F instrument. X-ray photoelectron spectroscopy (XPS) measurements were taken on a Gamdata-Scientia SES 2002 analyzer with a monochromatic Al K α X-ray source.

Electrochemical measurements

In our experiment, the linear sweep voltammetry (LSV), CV, electrochemical impedance spectroscopy (EIS) and stability test were performed at in the standard three-electrode system with 1 M KOH electrolyte (PINE, Grove City, America). All of the potentials were calibrated to RHE based on the Nernst equation. The scan rate of LSV measurements was 5 mV s⁻¹. The electrochemical active area (ECSA) was calculated by measurement of the capacitive current related to double-layer charging from the scan-rate dependence of CVs. The EIS measurement was performed over a frequency range from 100 kHz to 0.01 Hz at an open circuit potential, and the amplitude potential was 10 mV.

Results and discussion

The CNTs/N-Cu₂S nanocomposites were obtained via electrochemical deposition using CV in a three-electrode system, as illustrated in Fig. 1. In a typical experiment, TH was first uniformly distributed on the CNT surfaces by sonication. Subsequently, CV in an aqueous CuSO₄·5H₂O solution was used to grow Cu₂S on the CNTs-TH-modified GCE. Thiourea (H₂NCSNH₂) is commonly used as sulfur source to prepare metal sulfides because it has a strong tendency to coordinate with metallic cations and form semi-organic materials. The thiourea molecule may take effect mainly in two ways: (i) thiourea decomposes mildly and continuously to release S²⁻ under hydrothermal/solvothermal circumstances or even in common ambient conditions. The resulting S²⁻ ions then associate effectively with the metal cations to generate metal sulfide materials. (ii) thiourea could isomerize into ammonium thiocyanate, employing metal thiocyanate as the intermediate product. In the next step, CuSCN formed and then transformed into Cu₂S (Fang et al. 2013). The morphologies and compositions of the as-grown catalysts were determined by SEM, TEM and EDX. The SEM and TEM images of the CNTs/N-Cu₂S-5cyc catalyst (Fig. 2a-c; Fig. S1) showed that nanoscale clusters consisted of particles were uniformly distributed on the CNT surfaces (Fig. S2a and S2b). STEM was used to characterize the elemental distributions of the CNTs/N-Cu₂S-5cyc products, and the elemental maps of the CNTs/N-Cu₂S-5cyc (inset to Fig. 2d) demonstrated the homogeneous distribution of C, N, O, S and Cu throughout the material. The EDS analysis also determined that the CNTs/N-Cu₂S-5cyc was composed of C, N, O, S and Cu (Fig. S3). To examine the structure in more detail, SAED patterns of the material were acquired (Fig. 2c). These patterns exhibited a series of diffraction rings that can be ascribed to crystalline Cu₂S, indicating the polycrystalline structure of the product. HRTEM image (inset to Fig. 2d) also showed lattice fringes with spacings of 0.36 and 0.30 nm, corresponding to the (212) and (101) planes of Cu₂S, respectively. These results confirmed that Cu₂S clusters were successfully grown on the surfaces of the CNTs.

The chemical compositions and states of the catalyst materials were further evaluated by XPS, calibrating the binding energies relative to that of C 1s (284.6 eV). In Fig. 3a and Fig. S4, the XPS spectra of the as-grown products (made with different numbers of

electrodeposition cycles) indicate the presence of Cu, S, C, O and N. The high-resolution Cu 2p spectrum in Fig. 3b contains two prominent peaks, at 932.5 and 952.5 eV, that can be assigned to Cu 2p_{3/2} and Cu 2p_{1/2} and are characteristic of Cu₂S, which is consistent with previous reports (An et al. 2015; Wang et al. 2012; Lee et al. 2007; Schneider et al. 2007). The high-resolution S 2p spectrum in Fig. 3c, obtained from the catalyst prior to use in the OER, exhibits a wide peak from 161 to 166 eV. This region can be deconvoluted to give two peaks, corresponding to S 2p_{1/2} and S 2p_{3/2} (Wang et al. 2012; Lee et al. 2007; Schneider et al. 2007), which appear at positions very close to those produced by thiourea (162.3 eV) and so confirm the presence of S²⁻ ions. The CNTs/Cu₂S-N-5cyc also produced an XPS peak at approximately 168 eV and that can be ascribed to SO₄²⁻ resulting from the CuSO₄ solution used during the electrochemical deposition. The high-resolution N 1s spectra in Fig. 3d indicate no significant differences in the positions of the N 1s peaks produced by thiourea (400 eV) and the CNTs/N-Cu₂S-5cyc (399.8 eV) prior to the OER. These results can be attributed to the persistence of some portion of the N in the thiourea in the composite following the electrodeposition process. Together with the elemental maps (inset to Fig. 2d), these data confirm that CNTs/N-Cu₂S composites were successfully prepared via the electrodeposition method. The particles obtained by this N doping are expected to act as active sites in electrocatalytic reactions (Zhang et al. 2017). The compositional ratio of each element in CNTs/N-Cu₂S hybrids was given in Table S1 according to XPS results.

The OER activity of the CNTs/N-Cu₂S-5cyc was assessed by systematic electrochemical investigations in the 1 M KOH electrolyte solution. For comparison, similar measurements were conducted with IrO₂, CNTs/CuO-5cyc, CNTs-TH and CNTs as the working electrode, and the resulting OER polarization curves are provided in Fig. 4a. It is evident that the CNTs/N-Cu₂S-5cyc catalyst produced an earlier onset potential of approximately 1.44 V (vs. RHE), and this value was slightly lower than that of the IrO₂ catalyst. However, the onset potentials of the CNTs/CuO-5cyc and CNTs-TH were 1.57 and 1.59 V (vs. RHE), respectively. As shown in Fig. 4a, the current density obtained from the CNTs/N-Cu₂S-5cyc composite was higher than those associated with the CNT-based catalysts (CNTs, CNTs-TH and CNTs/CuO-5cyc). The CNTs/N-Cu₂S-5cyc also delivered an overpotential of only 280 mV at a current density of

10 mA cm⁻², which was much smaller than those generated by the CNTs/CuO-5cyc (380 mV), CNTs-TH (420 mV) and CNTs (430 mV). The data in Table 1 indicate that the CNTs/N-Cu₂S-5cyc catalyst displayed the best overall OER catalytic activity and that this performance was comparable with values reported for other catalysts in the literature (Table S2) (Yu et al. 2017; He et al. 2018; Liang et al. 2018; Wu et al. 2018; Xu et al. 2016a, b). Thus, the CNTs/N-Cu₂S-5cyc composite was evidently a highly active OER catalyst.

A Tafel curve shows the linear relationship between the current density and overpotential values and can be used to evaluate the kinetics and activity of these materials when used as OER catalysts (Wei et al. 2019). The Tafel slope is obtained by fitting the polarization curve to the Tafel equation ($\eta = b \log(j) + c$), where j is the current density, b is the slope, η is the overpotential and c is a constant (Zhou et al. 2014; Zhou et al. 2015). The OER kinetics are inversely correlated with b , such that a lower value of b indicates a more efficient reaction. The Tafel plots are displayed in Fig. 4b, and the associated values are summarized in Table 1. The Tafel slope of 63 mV dec⁻¹ determined for the CNTs/N-Cu₂S-5cyc catalyst was much smaller than those for the IrO₂ (71 mV dec⁻¹), CNTs/CuO-5cyc (94 mV dec⁻¹), CNTs-TH (145 mV dec⁻¹) and CNTs (158 mV dec⁻¹). The Tafel slope of the CNTs/N-Cu₂S-5cyc was also significantly lower than those previously reported for catalysts based on Cu and other non-precious metals (Zhou et al. 2015; Zhou et al. 2014; Chauhan et al. 2017; Zhang et al. 2018; Xu et al. 2016a, b; Yang et al. 2017a, b) (see Table S2), reflecting the superior OER kinetics of this new material.

The above experimental results and data analysis demonstrate the improved catalytic properties of the CNTs/N-Cu₂S-5cyc stemming from the addition of thiourea. The data obtained from CNTs/CuO-5cyc catalysts synthesized without TH are shown (Fig. 5, Fig. S2e and S2f). These results demonstrate the non-uniform growth of disordered cubic CuO crystals on the CNT surfaces. The average size of the crystals in these samples was approximately 600 nm, which is much larger than that of the Cu₂S particles in Fig. 2. The elemental map of the CNTs/CuO-5cyc (Fig. 5b) also shows homogeneous distributions of C, O and Cu. The HRTEM images of this material (Fig. 5c, d) also show lattice fringes with spacings of 0.23, 0.25, 0.18 and 0.28 nm, corresponding to the (111), (002), (112) and (-110) planes of CuO, respectively, while the SAED pattern (inset Fig. 5d)

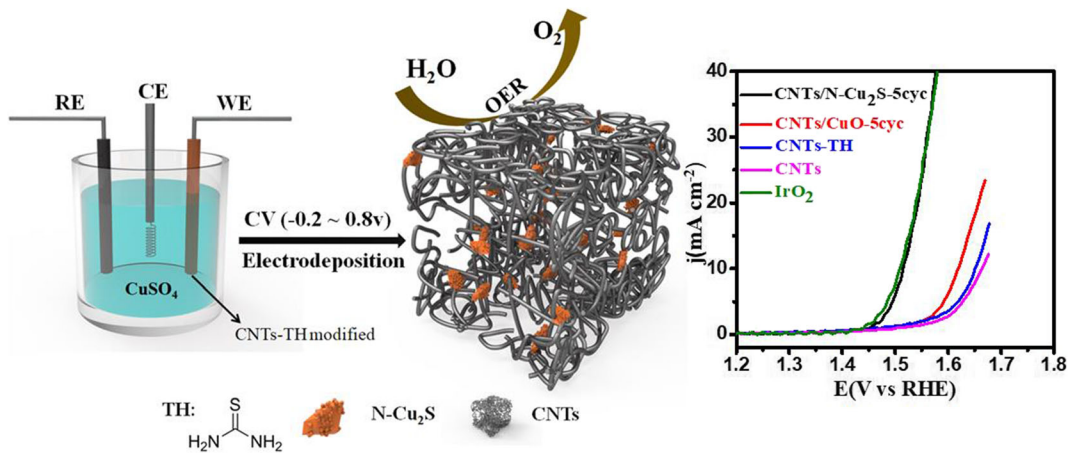
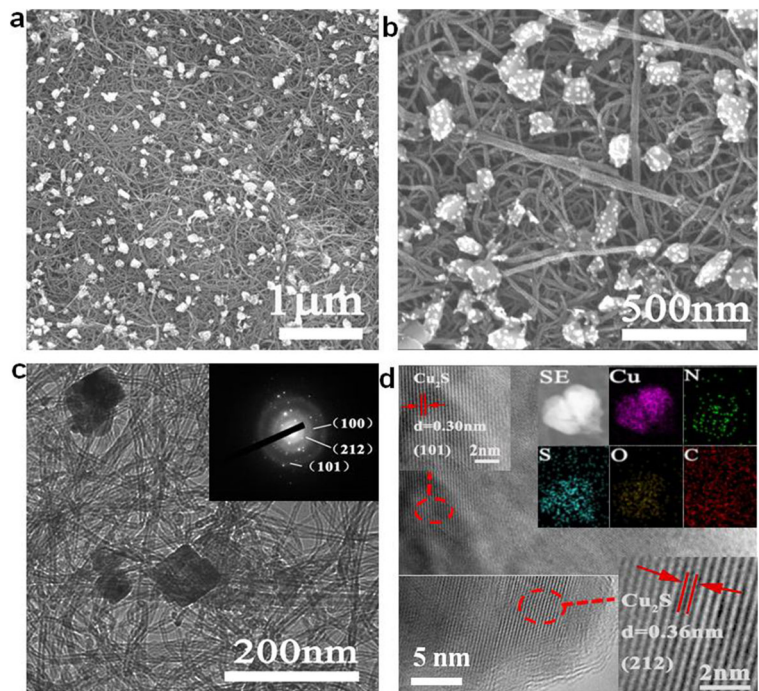


Fig. 1 A schematic diagram to illustrate the operating principle of the OER based on CNTs/N-Cu₂S nanocomposites by electrodeposition

exhibits a series of diffraction rings that can be ascribed to crystalline CuO (Wang et al. 2002; Park et al. 2009; Cao et al. 2003). These results indicate that the intended CNTs/CuO-5cyc composites were successfully obtained (Fig. 6e, f; Fig. S5) present XPS spectra of the CNTs/CuO-5cyc and confirm the presence of Cu, C and O. The Cu 2p peaks with satellites located at higher binding energies in these spectra confirm the Cu²⁺ valence state in the CNTs/CuO-5cyc compared with that of the CNTs/N-Cu₂S-5cyc composite (Morales et al. 2005; Hsieh et al. 2003). In addition, both the CNTs/N-

Cu₂S-5cyc and CNTs/CuO-5cyc catalysts produced an XPS peak at approximately 169 eV corresponding to sulfur oxide due to the CuSO₄ solution used in the electrochemical deposition. These results demonstrate that the thiourea was uniformly fixed on the CNT surfaces and also provided a source of N and S, to produce homogeneous CNTs/N-Cu₂S composites. This uniform doping of N should produce numerous active sites that improve the OER performance. To confirm this, the catalytic performances obtained from materials with different mass ratios of CNTs and thiourea under the

Fig. 2 Structural characterization of as-synthesized CNTs/N-Cu₂S-5cyc hybrid catalysts: **a** and **b** SEM images. **c** TEM images (the inset of SAED) and **d** corresponding elemental mapping and HRTEM



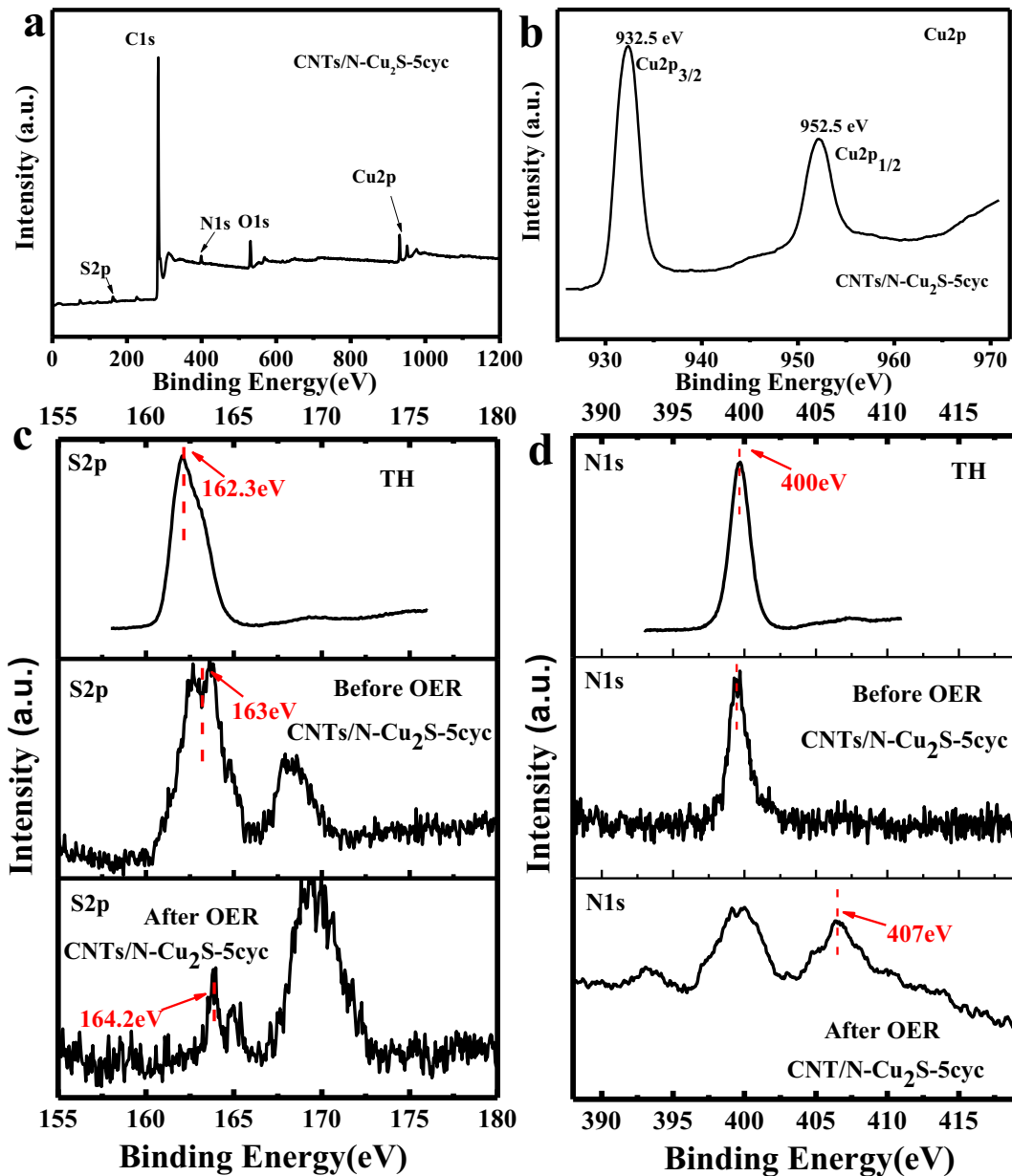


Fig. 3 a XPS spectra survey of the CNTs/N-Cu₂S-5cyc. b High-resolution XPS spectra of Cu 2p. c the S 2p of TH and CNTs/N-

Cu₂S-5cyc (before and after OER). d the N 1s of TH and CNTs/N-Cu₂S-5cyc (before and after OER), respectively

same electrodeposition conditions were assessed. As shown in Fig. S6, the OER performance of the sample containing a CNTs:TH ratio of 4 mg:4 mg was better than those of the 2 mg:4 mg, 3 mg:4 mg and 5 mg:4 mg specimens. These results can be ascribed to the poor conductivity produced by the use of an excessive amount of thiourea or the fewer active sites when using less thiourea. Therefore, thiourea played a key role in

the preparation of these N-doped Cu-based composites by acting as a source of both N and S. The 4 mg:4 mg specimen exhibited the best catalytic performance and so was used in the subsequent experiments.

During the process of electrochemical deposition by CV, the quantity of electrodeposition cycles, the potential range and the scan rate were found to greatly affect the performance of the as-prepared catalysts in a fuel

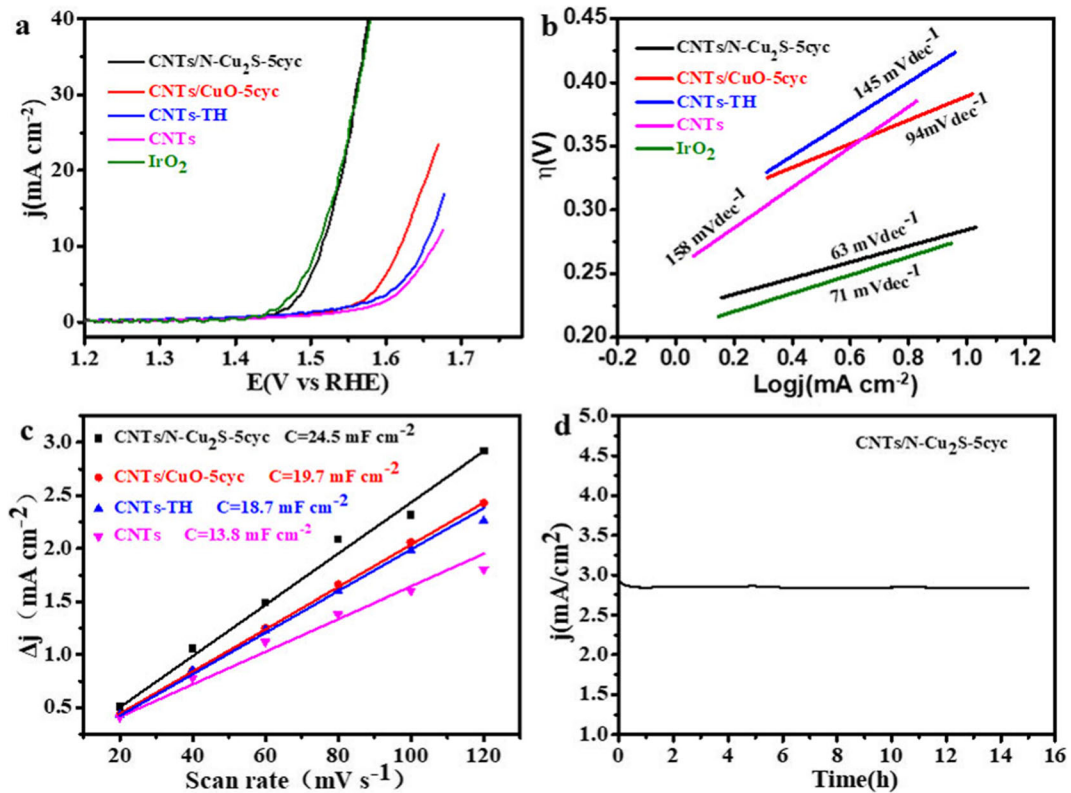


Fig. 4 Electrochemical catalytic performance of as-grown catalysts. **a** Linear sweep voltammograms of all catalytic electrodes in 1 M KOH with 95% iR corrections. **b** Tafel plots of all catalysts loaded on GCE recorded in 1 M KOH, corresponding to the LSV

curves in Fig. 4a. **c** Charging current density differences plotted versus scan rate. The linear slope, equivalent to twice the double-layer capacitance C_{dl} , was used to represent the ECSA. **d** Chronoamperometric curve of CNTs/N-Cu₂S-5cyc in 1 M KOH

cell. Hence, the effects of the number of electrodeposition cycles, the potential range and the scan rate were systematically investigated. The synthesis conditions of the potential range and scan rate were listed in the Table S3 and the SEM images of CNTs/N-Cu₂S-5cyc (1), CNTs/N-Cu₂S-5cyc (2), CNTs/N-Cu₂S-5cyc (3) and CNTs/N-Cu₂S-5cyc (4) were given in Fig. S7. It was found from Fig. S8 that the catalytic performance of

CNTs/N-Cu₂S-5cyc is better than those of CNTs/N-Cu₂S-5cyc (1) and CNTs/N-Cu₂S-5cyc (2) with different potential range. Herein, we chose the CNTs/N-Cu₂S-5cyc (potential range: + 0.8 V to - 0.6 V) in the subsequent experiments. CNTs/N-Cu₂S-5cyc (3) and CNTs/N-Cu₂S-5cyc (4) catalysts showed much lower current densities than that of CNTs/N-Cu₂S-5cyc (Fig. S8), which could be attributed that low scan rate resulted

Table 1 Summary of catalytic parameters of different OER catalysts

Samples	onset (V vs. RHE)	(mV) @ 10 mA cm ⁻²	(mV) @ 20 mA cm ⁻²	Tafel slope (mV dec ⁻¹)	Capacitance (mF cm ⁻²)
CNTs/N-Cu ₂ S-3cyc	1.46	300	330	86	17.97
CNTs/N-Cu ₂ S-5cyc	1.44	280	310	63	24.5
CNTs/N-Cu ₂ S-10cyc	1.47	360	400	133	17.5
CNTs/N-Cu ₂ S-15cyc	1.51	390	430	145	14.06
CNTs-CuO-5cyc	1.57	380	420	94	19.7
CNTs-TH	1.59	420	460	145	18.7
CNTs	1.60	430	490	158	13.8

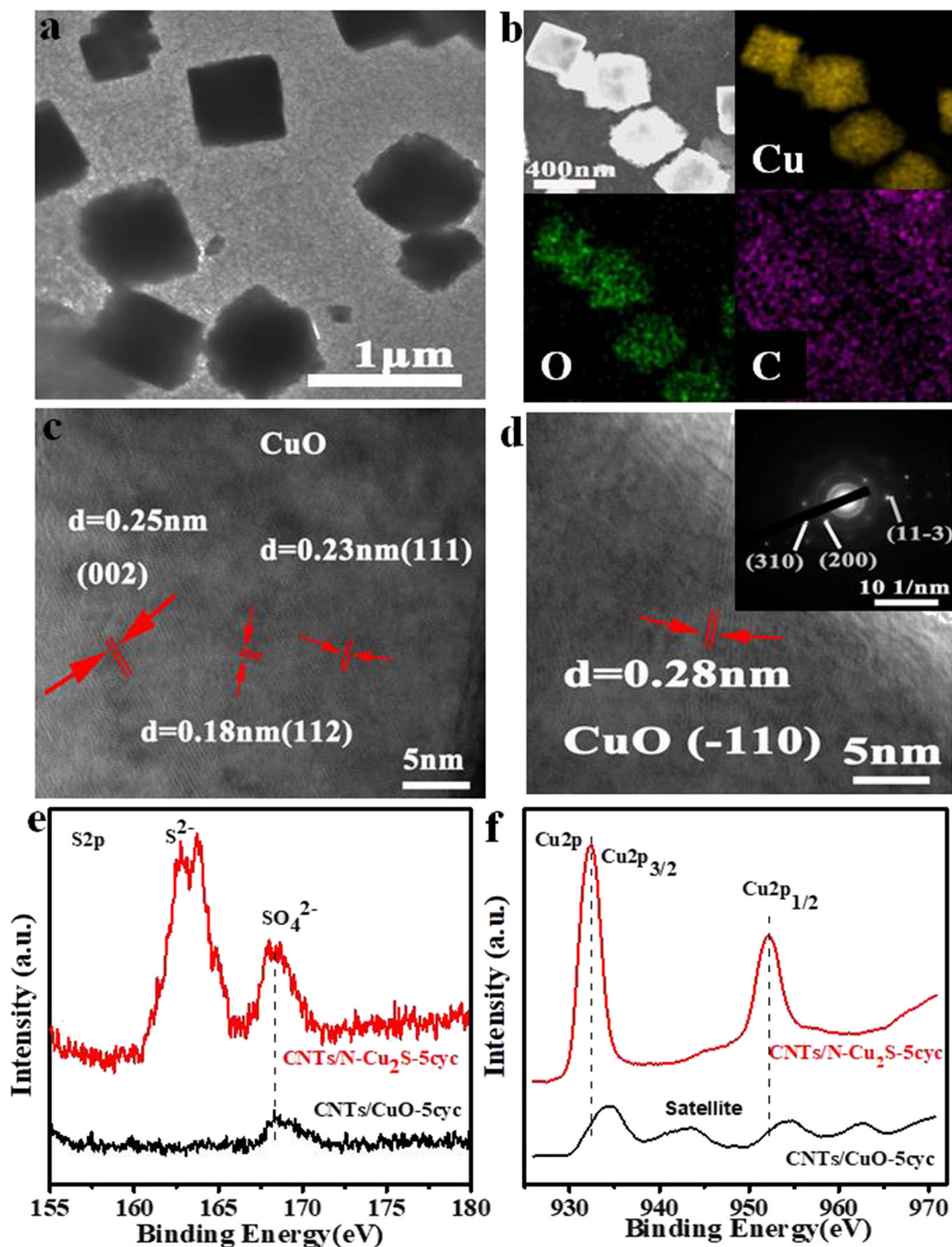


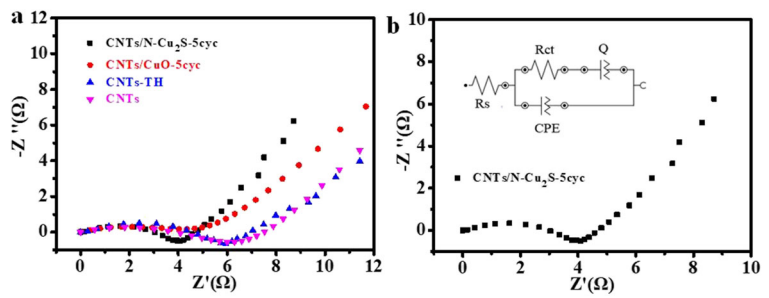
Fig. 5 Characterizations of the CNTs/CuO-5cyc materials. **a** TEM images. **b** Element mapping images. **c** and **d** HRTEM (inset the SAED). **e** XPS spectra survey of the S 2p of CNTs/CuO-5cyc

and CNTs/N-Cu₂S-5cyc. **f** The Cu 2p of CNTs/CuO-5cyc (before the OER) and CNTs/N-Cu₂S-5cyc (before the OER)

in the low reaction during the process of electrochemical deposition. SEM images (Fig. S7) also reflected the phenomenon that CNTs/N-Cu₂S-5cyc (4) with fast scan

rate displayed large particles during the fast process of electrochemical deposition. Hence, the CNTs/N-Cu₂S-5cyc (scan rate: 40 mV s⁻¹) was used in the subsequent

Fig. 6 **a** Impedance Nyquist plots of all catalysts in KOH electrolyte solution. **b** The measured curves of CNTs/N-Cu₂S-5cyc (inset equivalent circuit models OH⁻/O₂ of CNTs/N-Cu₂S-5cyc) in 1 M KOH. **c** The table for the detailed parameters of EIS



Samples	Rs/Ω	Rct/Ω	CPE/μMho	Q/μMho
CNTs-TH-Cu-3cyc	49.0	9.71	19.8	435
CNTs-TH-Cu-5cyc	18.4	6.77	45.1	312
CNTs-TH-Cu-10cyc	44	7.56	19.2	394
CNTs-TH-Cu-15cyc	70.9	9.36	23.2	340
CNTs-Cu-5cyc	19.5	8	127	442
CNTs-TH	19.0	9.51	38.1	371
CNTs	20.9	10.2	16.2	504

experiments SEM images of the CNTs/N-Cu₂S-3cyc, CNTs/N-Cu₂S-10cyc and CNTs/N-Cu₂S-15cyc specimens are shown in Fig. S9. The CNTs/Cu₂S-3cyc image exhibits a small amount of nanoclusters scattered over the CNTs as a result of the electrochemical deposition. These structures may produce insufficient active sites. The CNTs/N-Cu₂S-10cyc and CNTs/N-Cu₂S-15cyc catalysts show dense, compact particle accumulation encompassing the CNTs, which could serve to block active sites and reduce the catalytic efficiency. From Fig. S10a, Fig. S10b and Table 1, it is apparent that the CNTs/N-Cu₂S-5cyc catalyst displayed the best OER catalytic activity together with a low overpotential at specific current densities and a lower Tafel slope compared with those for the CNTs/N-Cu₂S-3cyc, CNTs/N-Cu₂S-10cyc and CNTs/N-Cu₂S-15cyc catalysts. The morphological analysis of these composites (Fig. S9) shows a lack of efficient active sites on the CNTs/N-Cu₂S-3cyc composite owing to the use of fewer electrodeposition cycles. However, the active sites on the CNTs/N-Cu₂S-10cyc and CNTs/N-Cu₂S-15cyc composites were likely covered due to the greater number of electrodeposition cycles. Hence, these results further confirm that the CNTs/N-Cu₂S-5cyc catalyst would be expected to afford satisfactory OER performance.

The CNTs/N-Cu₂S-5cyc catalyst is believed to have shown enhanced electrochemical catalysis of the OER for several reasons. A high active surface area is an important requirement for an OER catalyst, and so an increase in the

active surface area typically improves the catalytic activity (Yang et al. 2017a, b). The electrochemical C_{dl} values were determined to assess the surface areas because this value reflects the interface between the solid electrode and the electrolyte, which, in turn, is affected by the distribution of charge at the interface. The ECSA values were estimated based on the CV data and the C_{dl} of the materials, as shown in Fig. 4c and Fig. S10c, S11 and S12 and the data in Table 1 demonstrate that the CNTs/N-Cu₂S-5cyc had the highest C_{dl} out of the various samples studied, with a value of 24.5 mF cm⁻². Therefore, the surface of this material had more exposed active sites compared with the CNTs/CuO-5cyc (19.7 mF cm⁻²), CNTs-TH (18.7 mF cm⁻²) and CNTs (13.8 mF cm⁻²) during the OER process. Consequently, the CNTs/N-Cu₂S-5cyc was more active because a greater surface area was available for electrolyte permeation, which, in turn, promoted the OER.

The improved electrocatalytic activity of the composite electrode demonstrated herein can also be attributed to the presence of the CNTs, which produced synergistic interactions at their interfaces. Additional information regarding the interfacial properties and ohmic losses of the electrode during the OER process was obtained by EIS of the catalysts held at the same potential in alkaline solutions. The resulting Nyquist plots are presented in Fig. 6a and b, Fig. S10d, while the impedance parameters obtained by fitting the EIS responses are shown in Fig. 6c. The inset to Fig. 6b also

provides the equivalent electrical circuit diagram. The CNTs/N-Cu₂S-5cyc was found to possess a relatively low charge transfer resistance (R_{ct} ; 6.77 Ω) and low solution resistance (R_s ; 18.4 Ω), along with the highest capacitance (CPE) value among the various catalysts. While the CNTs/N-Cu₂S-10cyc and CNTs/N-Cu₂S-15cyc electrodes displayed higher charge transfer resistance (7.56 Ω and 9.36 Ω , respectively), which may be due to the comparatively high Cu₂S content and may result in a decrease in the interface area between the CNTs and the electrolyte, which would increase the resistance for the CNTs/N-Cu₂S-10cyc and CNTs/N-Cu₂S-15cyc electrodes, consistent with the morphologies of them (Fig. S9). The low R_s and R_{ct} values of this material indicate faster surface charge transfer and a higher reaction rate between the electrode and electrolyte interface. In addition, the large CPE value (45.1 Ω) corresponds to a high active surface area. These results demonstrate that the CNTs/Cu₂S-N-5cyc exhibits improved conductivity as a result of its lower R_{ct} , which, in turn, boosts the catalytic activity.

The valence states of Cu cations are of great importance to the OER. The valence state conversion of Cu cations can enhance the electrophilicity of adsorbed O, thus promoting the formation of hydroperoxy (–OOH) species and the subsequent evolution of O₂ (An et al. 2015). However, in the present work, the CNTs/N-Cu₂S-5cyc catalyst exhibited a higher current density than that obtained from the CNTs/CuO-5cyc (Fig. 4a; Table 1). This could be related to the unique properties of N-doped Cu₂S nanoparticles, which can undergo a change in oxidation state during the OER similar to that of cobalt oxide (Wu et al. 2015; Xu et al. 2016b; Cai et al. 2017). In the XPS data obtained from the CNTs/N-Cu₂S-5cyc catalyst after OER trials (Fig. S13), the Cu 2p_{2/3} peak indicates a higher valence state, in agreement with previous reports regarding the use of Cu-based catalysts in the OER (Li et al. 2017). Based on Fig. 3c and d, it is likely that N and S also play a role in the OER processes.

In addition to high catalytic activity, long-term operating stability is also essential for practical applications. For this reason, the stability of a CNTs/N-Cu₂S-5cyc electrode was assessed by chronoamperometric analysis with a 1.55 V (vs. RHE) bias in a 1 M KOH solution. As shown in Fig. 4d, a stable reaction was maintained for approximately 15 h, and no appreciable deactivation was observed over this time span, demonstrating that the catalyst was suitably durable.

Conclusion

A facile electrochemical deposition method was used to prepare composites consisting of CNTs and Cu₂S clusters. The CNTs functioned as a conductive substrate to improve the electrical conductivity of the Cu₂S and thus enhance charge transport. Clusters of small N-Cu₂S particles were formed that increased the surface area and created more active sites. These, in turn, raised the OER catalytic activity. The CNTs/N-Cu₂S-5cyc catalyst displayed excellent catalytic performance, with a current density of 10 mA cm⁻² at a low OER overpotential of 280 mV, a low Tafel slope of 63 mV dec⁻¹ and the significant electrochemical stability in the 1.0 M KOH solution. To our knowledge, these results are among the best yet reported for Cu-based OER catalysts in alkaline conditions, suggesting a promising alternative to noble metals in future clean energy technologies.

Acknowledgments We thank Michael D. Judge, MSc, from Liwen Bianji, Edanz Editing China (www.liwenbianji.cn/ac), for editing the English text of a draft of this manuscript.

Funding information The work was supported in part by grants from National Natural Science Foundation of China (51972238, 21875166, 51741207, 21475096 and 51572197) and China post-doctoral science foundation (2017M622630), Natural Science Foundation of Zhejiang Province (LR18E020001), Science and Technology Project of Zhejiang Province (LGF18B050005).

Compliance with ethical standards

Conflict of interest The authors declare that they have no conflict of interest.

References

- An L, Zhou P, Yin J, Liu H, Chen F, Liu H, Du Y, Xi P (2015) Phase transformation fabrication of a Cu₂S nanoplate as an efficient catalyst for water oxidation with glycine. *Inorg Chem* 54:3281–3289
- Brimblecombe R, Koo A, Dismukes GC, Swiegers GF, Spiccia L (2010) Solar driven water oxidation by a bioinspired manganese molecular catalyst. *J Am Chem Soc* 132:2892–2894
- Cai P, Huang J, Chen J, Wen Z (2017) Oxygen-containing amorphous cobalt sulfide porous nanocubes as high-activity electrocatalysts for the oxygen evolution reaction in an alkaline/neutral medium. *Angew Chem Int Ed* 129:4936–4939
- Cao M, Hu C, Wang Y, Guo Y, Guo C, Wang E (2003) A controllable synthetic route to Cu, Cu₂O, and CuO nanotubes and nanorods. *Chem Commun* 15:1884–1885

- Chauhan M, Reddy KP, Gopinath CS, Deka S (2017) Copper cobalt sulfide nanosheets realizing a promising electrocatalytic oxygen evolution reaction. *ACS Catal* 7:5871–5879
- Chen P, Xu K, Zhou T, Tong Y, Wu J, Cheng H, Lu X, Ding H, Wu C, Xie Y (2016) Strong-coupled cobalt borate nanosheets/graphene hybrid as electrocatalyst for water oxidation under both alkaline and neutral conditions. *Angew Chem Int Ed* 55: 2488–2492
- Dou S, Tao L, Huo J, Wang S, Dai L (2016) Etched and doped Co_9S_8 /graphene hybrid for oxygen electrocatalysis. *Energy Environ Sci* 9:1320–1326
- Fang Z, Wang C, Fan F, Hao S, Long L, Song Y, Qiang T (2013) Phase evolution of Cu-S system in ethylene glycol solution: the effect of anion and PVP on the transformation of thiourea. *Chin J Chem* 31:1015–1021
- Guo Y, Tong Y, Chen P, Xu K, Zhao J, Lin Y, Chu W, Peng Z, Wu C, Xie Y (2015) Engineering the electronic state of a perovskite electrocatalyst for synergistically enhanced oxygen evolution reaction. *Adv Mater* 27:5989–5994
- He L, Zhou D, Lin Y, Ge R, Hou X, Sun X, Zheng C (2018) Ultrarapid in situ synthesis of Cu_2S nanosheet arrays on copper foam with room-temperature-active iodine plasma for efficient and cost-effective oxygen evolution. *ACS Catal* 8:3859–3864
- Hsieh C-T, Chen J-M, Lin H-H, Shih H-C (2003) Field emission from various CuO nanostructures. *Appl Phys Lett* 83: 3383–3385
- Kanan MW, Surendranath Y, Nocera DG (2009) Cobalt-phosphate oxygen-evolving compound. *Chem Soc Rev* 38: 109–114
- Ku G, Zhou M, Song S, Huang Q, Hazle J, Li C (2013) Copper sulfide nanoparticles as a new class of photoacoustic contrast agent for deep tissue imaging at 1064 nm. *ACS Nano* 6:7489
- Lee H, Yoon SW, Kim EJ, Park J (2007) In-situ growth of copper sulfide nanocrystals on multiwalled carbon nanotubes and their application as novel solar cell and amperometric glucose sensor materials. *Nano Lett* 7:778–784
- Li J, Yan M, Zhou X, Huang ZQ, Xia Z, Chang CR, Ma Y, Qu Y (2016) Mechanistic insights on ternary $\text{Ni}_{2-x}\text{Co}_x\text{P}$ for hydrogen evolution and their hybrids with graphene as highly efficient and robust catalysts for overall water splitting. *Adv Funct Mater* 26:6785–6796
- Li Q, Wang X, Tang K, Wang M, Wang C, Yan C (2017) Electronic modulation of electrocatalytically active center of Cu_2S_4 nanodisks by cobalt-doping for highly efficient oxygen evolution reaction. *ACS Nano* 11:12230–12239
- Li H, Wang K, Cheng S, Jiang K (2018) Controllable electrochemical synthesis of copper sulfides as sodium-ion battery anodes with superior rate capability and ultralong cycle life. *ACS Appl Mater Interfaces* 10:8016–8025
- Liang H, Shuang W, Zhang Y, Chao S, Han H, Wang X, Zhang H, Yang L (2018) Graphene-like multilayered CuS nanosheets assembled into flower-like microspheres and their electrocatalytic oxygen evolution properties. *ChemElectroChem* 5: 494–500
- Liu Y, Xiao C, Lyu M, Lin Y, Cai W, Huang P, Tong W, Zou Y, Xie Y (2015) Ultrathin Co_3S_4 nanosheets that synergistically engineer spin states and exposed polyhedra that promote water oxidation under neutral conditions. *Angew Chem Int Ed* 127:11383–11387
- Morales J, Espinos J, Caballero A, Gonzalez-Elipe A, Mejias JA (2005) XPS study of interface and ligand effects in supported Cu_2O and CuO nanometric particles. *J Phys Chem B* 109: 7758–7765
- Nakagawa T, Bjorge NS, Murray RW (2009) Electrogenerated IrOx nanoparticles as dissolved redox catalysts for water oxidation. *J Am Chem Soc* 131:15578–15579
- Nocera DG (2012) The artificial leaf. *Chem Res* 45:767–776
- Over H (2012) Surface chemistry of ruthenium dioxide in heterogeneous catalysis and electrocatalysis: from fundamental to applied research. *Chem Rev* 112:3356–3426
- Park JC, Kim J, Kwon H, Song H (2009) Gram-scale synthesis of Cu_2O nanocubes and subsequent oxidation to CuO hollow nanostructures for lithium-ion battery anode materials. *Adv Mater* 21:803–807
- Schneider S, Ireland JR, Hersam MC, Marks TJ (2007) Copper (I) tert-butylthiolato clusters as single-source precursors for high-quality chalcocite thin films: film growth and microstructure control. *Chem Mater* 19:2780–2785
- Shen J, Yang Z, Ge M, Li P, Nie H, Cai Q, Gu C, Yang K, Huang S (2016) Neuron-inspired interpenetrative network composed of cobalt-phosphorus-derived nanoparticles embedded within porous carbon nanotubes for efficient hydrogen production. *ACS Appl Mater Interfaces* 8:17284–17291
- Subbaraman R, Tripkovic D, Chang K-C, Strmcnik D, Paulikas AP, Hirunsit P, Chan M, Greeley J, Stamenkovic V, Markovic NM (2012) Trends in activity for the water electrolyser reactions on 3d M (Ni, Co, Fe, Mn) hydr (oxy) oxide catalysts. *Nat Mater* 11:550
- Suen N-T, Hung S-F, Quan Q, Zhang N, Xu Y-J, Chen HM (2017) Electrocatalysis for the oxygen evolution reaction: recent development and future perspectives. *Chem Soc Rev* 46: 337–365
- Suntivich J, May KJ, Gasteiger HA, Goodenough JB, Shao-Horn Y (2011) A perovskite oxide optimized for oxygen evolution catalysis from molecular orbital principles. *Science* 334: 1383–1385
- Tanveer M, Cao C, Ali Z, Aslam I, Idrees F, Khan WS, But FK, Tahir M, Mahmood N (2014) Template free synthesis of CuS nanosheet-based hierarchical microspheres: an efficient natural light driven photocatalyst. *CrystEngComm* 16:5290
- Wang H, Xu J-Z, Zhu J-J, Chen H-Y (2002) Preparation of CuO nanoparticles by microwave irradiation. *J Cryst Growth* 244: 88–94
- Wang Y, Ai X, Miller D, Rice P, Topuria T, Krupp L, Kellock A, Song Q (2012) Two-phase microwave-assisted synthesis of Cu_2S nanocrystals. *CrystEngComm* 14:7560
- Wei C, Rao RR, Peng J, Huang B, Stephens I, Risch M, Shao-Horn Y (2019) Recommended practices and benchmark activity for hydrogen and oxygen electrocatalysis in water splitting and fuel cells. *Adv Mater* 31:1806296
- Wu L, Li Q, Wu CH, Zhu H, Mendoza-Garcia A, Shen B, Guo J, Sun S (2015) Stable cobalt nanoparticles and their monolayer array as an efficient electrocatalyst for oxygen evolution reaction. *J Am Chem Soc* 137:7071–7074
- Wu J-X, He C-T, Li G-R, Zhang J-P (2018) An inorganic-MOF-inorganic approach to ultrathin CuO decorated Cu-C hybrid nanorod arrays for an efficient oxygen evolution reaction. *J Mater Chem A* 6:19176–19181
- Xie L, Zhang R, Cui L, Liu D, Hao S, Ma Y, Du G, Asiri AM, Sun X (2017) High-performance electrolytic oxygen evolution in

- neutral media catalyzed by a cobalt phosphate nanoarray. *Angew Chem Int Ed* 56:1064–1068
- Xu H, Feng J-X, Tong Y-X, Li G-R (2016a) Cu₂O-Cu hybrid foams as high-performance electrocatalysts for oxygen evolution reaction in alkaline media. *Angew Chem Int Ed* 7:986–991
- Xu L, Jiang Q, Xiao Z, Li X, Huo J, Wang S, Dai L (2016b) Plasma-engraved Co₃O₄ nanosheets with oxygen vacancies and high surface area for the oxygen evolution reaction. *Angew Chem Int Ed* 55:5277–5281
- Yang D, Gao L, Yang JH (2017a) Facile synthesis of ultrathin Ni(OH)₂-Cu₂S hexagonal nanosheets hybrid for oxygen evolution reaction. *J. Power Sources* 359:52–56
- Yang J, Yang Z, Li LH, Cai Q, Nie H, Ge M, Chen X, Chen Y, Huang S (2017b) Highly efficient oxygen evolution from CoS₂/CNT nanocomposites via a one-step electrochemical deposition and dissolution method. *Nanoscale* 9:6886–6894
- Yu L, Zhou H, Sun J, Qin F, Yu F, Bao J, Yu Y, Chen S, Ren Z (2017) Cu nanowires shelled with NiFe layered double hydroxide nanosheets as bifunctional electrocatalysts for overall water splitting. *Energy Environ Sci* 10:1820–1827
- Zhang G, Wang P, Lu W-T, Wang C-Y, Li Y-K, Ding C, Gu J, Zheng X-S, Cao F-F (2017) Co nanoparticles/co, N, S tri-doped graphene templated from in-situ-formed co, S co-doped g-C₃N₄ as an active bifunctional electrocatalyst for overall water splitting. *Chem Mater* 9:28566–28576
- Zhang S, Sun Y, Liao F, Shen Y, Shi H, Shao M (2018) Co₉S₈-CuS-FeS trimetal sulfides for excellent oxygen evolution reaction electrocatalysis. *Electrochim Acta* 283:1695–1701
- Zhao X, Li L, Zhang Y, Zhang H, Wang Y (2017) Uniquely confining Cu₂S nanoparticles in graphitized carbon fibers for enhanced oxygen evolution reaction. *Nanotechnology* 28:345402
- Zhou X, Xia Z, Zhang Z, Ma Y, Qu Y (2014) One-step synthesis of multi-walled carbon nanotubes/ultra-thin Ni(OH)₂ nanoplate composite as efficient catalysts for water oxidation. *J Mater Chem A* 2:11799–11806
- Zhou X, Xia Z, Tian Z, Ma Y, Qu Y (2015) Ultrathin porous Co₃O₄ nanoplates as highly efficient oxygen evolution catalysts. *J Mater Chem A* 3:8107–8114

Publisher's note Springer Nature remains neutral with regard to jurisdictional claims in published maps and institutional affiliations.